KIX-Mediated Assembly of the CBP−CREB−HTLV-1 Tax Coactivator−Activator Complex†

Andrew C. Vendel, Steven J. McBryant, and Kevin J. Lumb*

Department of Biochemistry and Molecular Biology, Colorado State University, Fort Collins, Colorado 80523-1870

Received July 23, 2003; Revised Manuscript Received August 27, 2003

ABSTRACT: The HTLV-1 transcriptional activator Tax is required for viral replication and pathogenesis. In concert with human CREB, Tax recruits the human transcriptional coactivator and histone acetyltransferase p300/CBP to the HTLV-1 promoter. Here we investigate the structural features of the interaction between Tax and the KIX domain of p300/CBP. Circular dichroism spectroscopy, nuclear magnetic resonance chemical shift perturbation mapping, and sedimentation equilibrium analysis show that KIX binds a Tax subdomain corresponding to residues 59−98 of Tax (called Tax_{59-98}). Circular dichroism spectroscopy suggests that Tax_{59-98} is intrinsically disordered (natively unfolded) in isolation and adopts an ordered conformation upon binding KIX. The interaction is disrupted by a single amino acid variation of Tax_{59-98} in which leucine 68 is substituted with proline. Chemical shift perturbation mapping reveals that the Tax-binding surface of KIX is distinct from that utilized by CREB, and corresponds to the site of KIX that interacts with the human transcription factors c-Jun and mixed lineage leukemia protein (MLL). Sedimentation equilibrium analysis shows that Tax and the phosphorylated KID domain of CREB can simultaneously bind KIX to form a ternary 1:1:1 complex. The results provide a molecular description of the concerted recruitment of p300/CBP via the KIX domain by Tax and phosphorylated CREB during Tax-mediated gene expression.

HTLV-1[1] predominantly infects CD4+ T-cells and is the etiological agent of adult T-cell leukemia and of the neurological disorder tropical spastic paraparesis/HTLV-1-associated myelopathy (*1*). HTLV-1 replication and pathogenesis are dependent on the virally encoded transcriptional activator Tax (*2*−*4*). In addition to activating viral gene expression, Tax alters the expression of numerous cellular genes involved in cell cycle regulation and apoptosis (*2*−*4*). The interference of Tax with normal cellular processes likely contributes to the extensive modulation of the transcriptional profile of HTLV-1-infected lymphocytes (*5*) and to HTLV-1-associated pathogenesis (*2*−*4*).

Tax contributes to the activation of HTLV-1 genes by promoting the binding of human CREB at atypical CRE sites of the viral promoter (*2*−*4*) (Figure 1). Tax and CREB then cooperate to recruit the related but distinct human transcriptional coactivators p300 and CBP (*2*−*4*). The interaction between CREB and p300/CBP normally depends on CREB phosphorylation in a region of CREB called KID (*6*, *7*). In contrast, during Tax-mediated expression at both viral and host CRE-containing promoters, the requirement for CREB phosphorylation may be alleviated by Tax forming a molecular bridge between the bZIP region of CREB and p300/CBP (*8*, *9*) (Figure 1).

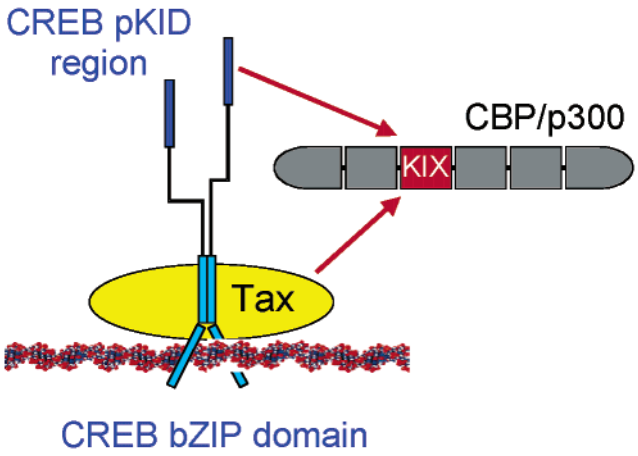

FIGURE 1: Schematic representation of the assembly of the CREB−Tax−CBP complex on DNA in the absence of CREB phosphorylation (*8*, *9*, *51*). In normal cells, the bZIP domain of CREB binds to the CRE. Upon phosphorylation, the KID region of CREB interacts with the KIX domain of the multidomain protein p300/CBP. During HTLV-1-mediated gene expression, Tax binds the bZIP region of CREB and contacts DNA to stabilize formation of the CREB−DNA complex at the atypical CRE sites of the HTLV-1 promoter. In the absence of KID phosphorylation, Tax binds KIX to act as a molecular bridge between the bZIP domain of CREB and p300/CBP (*8*, *9*).

The interaction between p300/CBP and Tax is mediated by the KIX domain of p300/CBP, as demonstrated by several *in vitro* and *in vivo* studies (*8*−*13*). The region of Tax that

† Supported by the American Cancer Society (Grant RSG-02-051-GMC).

* To whom correspondence should be addressed. E-mail: lumb@lamar.colostate.edu.

[1] Abbreviations: CBP, CREB-binding protein; CD, circular dichroism; CRE, cyclic AMP response element; CREB, CRE-binding protein; DSS, sodium 2,2-dimethyl-2-silapentane-5-sulfonate; HPLC, high-performance liquid chromatography; HSQC, heteronuclear single-quantum coherence; HTLV-1, human T-cell leukemia virus type 1; KID, kinase inducible domain of CREB; KIX, KID-interacting domain of CBP; LB, Luria-Bertani; MLL, mixed lineage leukemia protein; NMR, nuclear magnetic resonance; TFA, trifluoroacetic acid.

10.1021/bi0353023 CCC: $25.00
Published on Web 10/09/2003

binds KIX is localized in part to residues 76−95, since a peptide corresponding to residues 76−95 of Tax disrupts the association of full-length Tax and KIX *in vitro* (*10*).

Tax-mediated gene expression likely relies in part on the ability of p300 and CBP to interact with a range of host transcription factors (*14*) and the acetyltransferase chromatin remodeling activity of p300/CBP or the p300/CBP-associated factor (PCAF) (*12*, *13*). In addition to a role in HTLV-1 gene expression, p300 and CBP contribute to normal cellular processes such as cell growth, differentiation, and tumor progression (*15*, *16*). KIX interacts with numerous human transcription factors such as p53, MLL, c-Myb, and c-Jun (*15*, *16*). It is possible that competition for KIX between Tax and human transcription factors contributes to the development of HTLV-1-associated maladies (*17*−*19*).

KIX binds transcription factors via one of two modes that employ structurally distinct surfaces of KIX (*20*, *21*). One surface of KIX is recognized by the KID region of phosphorylated CREB (*22*), whereas a different surface is utilized by the human transcription factors c-Jun and MLL (*20*, *21*). The existence of two discrete binding sites on KIX allows the formation of ternary complexes with two activation domains (*20*, *21*). For example, KIX forms ternary complexes with the activation domains of CREB and MLL (*23*), of c-Myc and MLL (*21*), and of c-Jun and CREB (*20*).

Here we present an investigation of the Tax−KIX interaction and the formation of a ternary complex involving a domain of Tax corresponding to residues 59−98 (called Tax_{59-98}), the KIX domain of CBP, and the phosphorylated KID region of CREB. Tax_{59-98} is intrinsically disordered in isolation, and forms a stable complex with KIX. With NMR chemical shift perturbation mapping (*24*), we show that Tax_{59-98} binds to a contiguous site on KIX that corresponds to the site recognized by human c-Jun and MLL, and which is distinct from the binding site for CREB. In accord with the presence of two distinct binding sites for CREB and Tax, we show that KIX forms a ternary complex with Tax_{59-98} and phosphorylated KID. These results suggest a modified view of the assembly of the Tax−CREB−CBP complex during Tax-mediated gene expression in which ternary complex formation is facilitated by direct interactions between KIX and the phosphorylated KID region of CREB during p300/CBP recruitment.

EXPERIMENTAL PROCEDURES

Protein Preparation and Purification. Tax_{59-98}, corresponding to residues 59−98 of HTLV-1 Tax with an N-terminal Tyr for concentration determination, was synthesized on MBHA (4-methylbenzhydrylamine hydrochloride salt) resin (100−200 mesh) using manual Boc chemistry (*25*). The side chains of Arg, Asp, Gln, His, Lys, Ser, Thr, and Tyr were protected with Tos, Bzl, Xan, DNP, ClZ, Bzl, Bzl, and BrZ, respectively. Tax_{59-98} was purified by reversed phase C_{18} HPLC using a linear water/acetonitrile gradient containing 0.1% TFA. The identity of Tax_{59-98} was confirmed with electrospray mass spectrometry, and the observed and expected masses agreed to within 1 Da.

KIX (residues 589−679 of human CBP with an additional N-terminal Met) was expressed in *Escherichia coli* strain BL21(DE3) pLysS in LB medium and purified as described previously (*20*, *26*). ^{15}N-labeled KIX was prepared in the same way except cells were grown in M9 minimal medium supplemented with thiamine (*20*, *27*). Final purification was by reversed phase C_{18} HPLC using a linear water/acetonitrile gradient containing 0.1% TFA. The yield of KIX expressed in LB or M9 medium was typically 6 or 3 mg/L, respectively. The identity of KIX was confirmed with electrospray mass spectrometry, and the observed and expected masses agreed within 1 Da.

pKID corresponds to residues 87−143 of human CREB phosphorylated at Ser 118 (which is identical to residues 102−158 of mouse CREB phosphorylated at Ser133) with an additional N-terminal Met. Purified pKID was the generous gift of Y. Wei. KID was expressed in *E. coli* strain BL21(DE3) as a His-tagged fusion protein with a pET15b plasmid harboring a PCR product encoding KID amplified from a plasmid carrying human CREB-A (*28*) (S. P. Mestas and K. J. Lumb, unpublished results). KID was purified from the soluble cell lysate fraction with Ni affinity chromatography, and the His tag was cleaved with thrombin. KID was phosphorylated with protein kinase A (Sigma) (*7*). Final purification was accomplished by reversed phase C_{18} HPLC using a linear water/acetonitrile gradient containing 0.1% TFA. The identity of KIX was confirmed with MALDI mass spectrometry, and the observed and expected masses agreed within 1 Da.

Proteins were stored lyophilized and dialyzed against 20 mM sodium phosphate and 50 mM NaCl (pH 7.0) before being used.

Protein Concentration Determination. Concentrations of protein stock solutions were determined by absorbance in 6 M GuHCl, 10 mM sodium phosphate, and 150 mM NaCl, pH 6.5, at 25 °C using an extinction coefficient of 1450 M^{-1} cm^{-1} at 276 nm for Tax_{59-98} and pKID and of 12 090 M^{-1} cm^{-1} at 280 nm for KIX (*29*).

CD Spectroscopy. CD spectra were acquired with a Jasco J720 spectrometer. Samples were prepared in 20 mM sodium phosphate and 50 mM NaCl, pH 7.0, and contained equimolar amounts of each protein (20, 30, or 40 μM). Spectra comprised 20 scans recorded at 10 °C. Binding was detected by differences between observed spectra and the spectra expected if the two proteins do not interact, calculated as the normalized sum of the spectra of the individual proteins (*20*).

Analytical Ultracentrifugation. Sedimentation equilibrium analysis was performed with a Beckman XL-I analytical ultracentrifuge. Data were collected at 280 nm at the rotor speeds and protein concentrations listed in Table 1. Samples were dialyzed against the reference buffer (20 mM sodium phosphate and 150 mM NaCl, pH 7.0). Calculated partial specific volumes at 10 °C of 0.75, 0.71, 0.73, 0.72, 0.74, and 0.73 mL/g were used for Tax_{59-98}, pKID, KIX, pKID−KIX, Tax_{59-98}−KIX, and Tax_{59-98}−pKID−KIX, respectively (*30*). A calculated solvent density of 1.004 g/mL was used (*30*). Data were fit to an ideal, single-species model with ORIGIN (Beckman). Parameters that were allowed to float during the fit were the mass and the baseline offset (i.e., absorbance at c_0). Masses are reported as the mean of six observed masses ± the standard deviation.

NMR Spectroscopy. NMR spectra were acquired with a Varian Unity Inova spectrometer operating at 500.1 MHz for ^{1}H. All spectra were acquired at 10 °C. Samples were prepared in 20 mM sodium phosphate and 50 mM NaCl (pH

Table 1: Sedimentation Equilibrium Analysis of Binary and Ternary Complex Formation[a]

	observed mass (kDa)	
concentration (μM)	45 000 rpm	48 000 rpm
Tax_{59-98} (expected mass for monomer of 4607 Da)		
250	4.0	4.7
400	4.5	4.6
500	4.7	4.6
	observed mass (kDa)	
concentration (μM)	40 000 rpm	45 000 rpm
KIX (expected mass for monomer of 11 139.8 Da)		
40	11.7	11.4
50	11.7	11.5
60	11.8	12.1
	observed mass (kDa)	
concentration (μM)	45 000 rpm	48 000 rpm
pKID (expected mass for monomer of 6856 Da)		
200	7.1	7.6
300	6.9	6.8
400	7.0	7.0
	observed mass (kDa)	
concentration (μM)	25 000 rpm	30 000 rpm
pKID and KIX (expected mass for 1:1 complex of 17 996 Da)		
30	19.4	16.5
45	19.1	17.8
55	17.9	17.0
	observed mass (kDa)	
concentration (μM)	25 000 rpm	30 000 rpm
Tax_{59-98} and KIX (expected mass for 1:1 complex of 15 747 Da)		
37	14.2	13.1
50	14.2	12.6
62	13.0	13.3
	observed mass (kDa)	
concentration (μM)	25 000 rpm	30 000 rpm
Tax_{59-98}, pKID, and KIX (expected mass for 1:1:1 complex of 22 603 Da)		
35	23.0	21.3
45	21.0	21.5
55	20.2	21.8

[a] Data were collected at two rotor speeds and three concentrations. Samples contained the stated peptides in equimolar amounts with each peptide at the listed concentration.

7.0) and referenced to internal DSS at zero ppm. Gradient $^1H-^{15}N$ HSQC spectra (*31*) consisted of 256 complex increments defined by 192 transients and 1024 complex points. Data were processed with NMRPipe and analyzed with NMRView (*32*, *33*). Chemical shift assignments for the Tax_{59-98}−KIX complex were obtained by following changes in HSQC spectra of ^{15}N-labeled KIX (550 μM) upon addition of increasing amounts of unlabeled Tax_{59-98} (up to 1.1 mM). ^1H and ^{15}N assignments of unbound KIX have been previously reported (*20*). Changes in chemical shift ($\Delta\delta$) upon complex formation were calculated as $\sqrt{[(\Delta H^N)^2 + (\Delta N/5)^2]}$, where ΔH^N and ΔN are the changes in amide H^N and ^{15}N chemical shifts, respectively (*34*).

RESULTS

Tax_{59-98} Binds the KIX Domain of CBP. The CD spectrum of Tax_{59-98} is reminiscent of an unfolded protein, with a minimum at 200 nm and a lack of spectral characteristics above 210 nm that are reflective of helix or sheet structure (Figure 2). The CD spectrum of free KIX is indicative of a helical protein (Figure 2), in accord with previous CD results (*7*, *20*, *26*, *35*) and the solution structure of KIX (*22*). Addition of Tax_{59-98} to KIX results in a significant increase in ellipticity over the calculated spectrum of noninteracting Tax_{59-98} and KIX (Figure 2). This result suggests that Tax_{59-98} binds the KIX domain of CBP, in accord with previous studies of a shorter Tax peptide (*10*). In addition, the increase in ellipticity at the helical signature wavelengths of 208 and 222 nm suggests an increase in helix content upon binding.

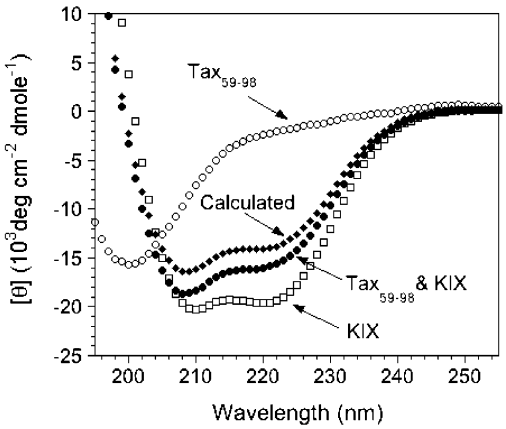

FIGURE 2: CD analysis of Tax_{59-98} binding to KIX. Mixing of Tax_{59-98} with KIX results in a CD spectrum with a negative ellipticity at 208 and 222 nm greater than that expected from the sum of the spectra of the two isolated proteins, suggesting that Tax_{59-98} binds KIX. Experiments were performed at three equimolar protein concentrations (20, 30, and 40 μM) in duplicate with reproducible results. From these six data sets, the error in the CD signal is estimated to be 2%. This error is significantly smaller than the difference of 20% at 222 nm between the calculated and observed spectra.

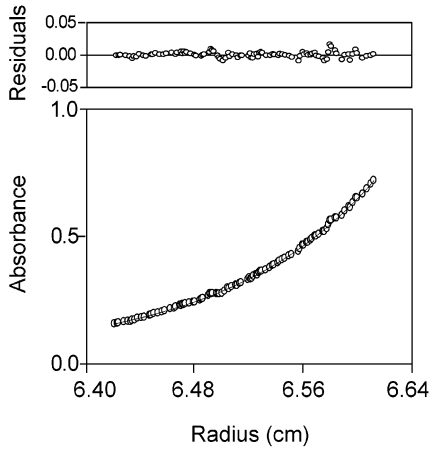

FIGURE 3: Sedimentation equilibrium analysis of binding of Tax_{59-98} to KIX. The data are consistent with an ideal, single-species model, as shown by the random distribution of residues.

Analytical ultracentrifugation also suggests that Tax_{59-98} and KIX interact (Figure 3). The apparent mass of equimolar Tax_{59-98} and KIX is 13.4 ± 0.3 kDa, which is within 15% of the mass of 15.7 kDa expected for the 1:1 complex (Table 1). If the complex did not form, then the apparent mass would reflect the weighted mass average of the individual proteins of 7.8 kDa. The lower-than-expected mass for the 1:1

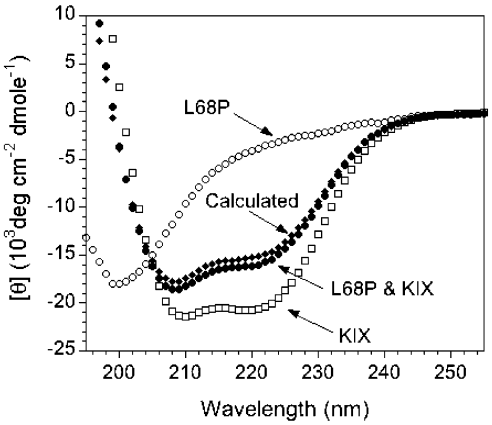

FIGURE 4: CD analysis of the L68P variant of Tax_{59-98}. Mixing of the L68P variant of Tax_{59-98} and KIX results in a CD spectrum that is very similar to the sum of the spectra of the two isolated proteins, suggesting that the L68P variant of Tax_{59-98} does not bind KIX.

complex may reflect error (for example, in the calculated partial specific volume), peptides that are not fully active, or incomplete formation of the complex, since 99% complex formation requires that the free ligand concentration be 100-fold greater than the K_d (*36*).

The observed mass of Tax_{59-98} does not vary systematically with concentration, as expected for a single species, and the mean mass of 4.5 ± 0.3 kDa is within 1% of the mass expected for a monomer of 4.6 kDa (Table 1). The observed mass for KIX of 11.7 ± 0.3 kDa is within 5% of the value expected for the monomer (Table 1), in accord with previous results (*20*). Thus, the observed mass of the equimolar solution of Tax_{59-98} and KIX is not the result of self-association of Tax_{59-98} or KIX as opposed to formation of the Tax_{59-98}−KIX complex.

A Single-Point Variant of Tax_{59-98} Disrupts KIX Binding. The CD results suggest an increase in helix content upon binding of Tax_{59-98} to KIX. Two regions of Tax_{59-98} are predicted with AGADIR (*37*) to have a propensity for helical formation (residues 60−71 and 83−89). If one of these two predicted helices is important for binding, then replacement of a potential hydrophobic interface residue with the secondary structure breaker proline (*38*) might be expected to disrupt binding. The L68P variant of Tax_{59-98} did not bind KIX as monitored with CD spectroscopy (Figure 4) or with NMR spectroscopy by changes in the $^1H-^{15}N$ HSQC spectrum of ^{15}N-labeled KIX upon the addition of the L86P variant (data not shown). This result provides evidence for a specific interaction between Tax_{59-98} and KIX.

NMR Mapping of the Tax_{59-98}-Binding Surface of KIX. The Tax_{59-98}-binding surface of KIX was identified by monitoring chemical shift changes in HSQC spectra of ^{15}N-labeled KIX upon the addition of increasing amounts of unlabeled Tax_{59-98} at neutral pH (Figure 5). Although absolute changes in chemical shift cannot usually be interpreted in detailed structural terms, residues that from a contiguous surface of a protein upon formation of a complex map the recognition interface of the protein−protein complex (*24*). Tax_{59-98} induces progressive changes in the ^1H and ^{15}N chemical shifts of KIX, indicating that complex formation is in the fast exchange regime on the chemical shift time scale. The average change in chemical shift upon formation

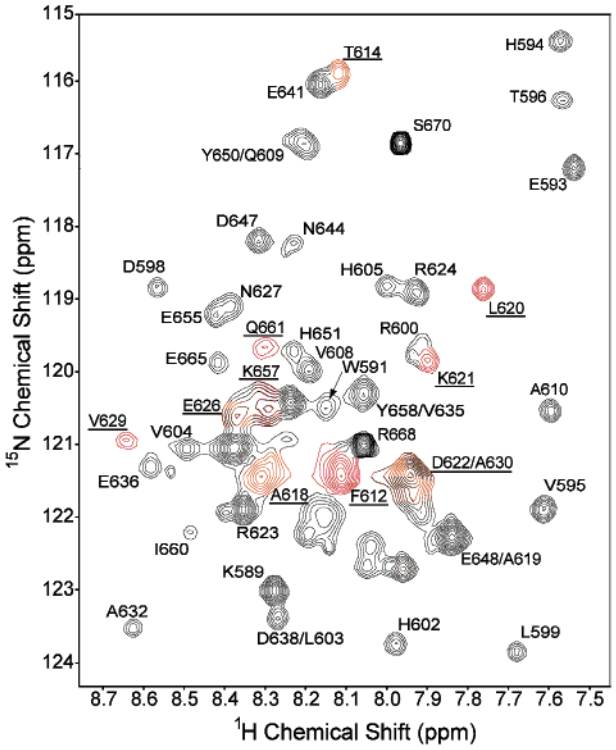

FIGURE 5: $^1H-^{15}N$ HSQC spectrum of ^{15}N-labeled KIX bound to Tax_{59-98} (10 °C, pH 7.0). Only resonances from ^{15}N-labeled KIX are observed in this experiment. KIX resonances that have a significant chemical shift perturbation upon binding Tax_{59-98} are colored orange ($\Delta\delta$ > 0.05 ppm) or red ($\Delta\delta$ > 0.08 ppm).

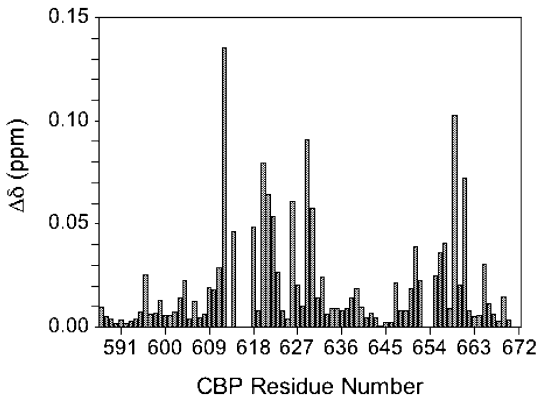

FIGURE 6: Chemical shift perturbations ($\Delta\delta$) induced in KIX by Tax_{59-98}. Changes are normalized averages of the amide H^N and N chemical shift perturbations (*34*).

of the Tax_{59-98}−KIX complex is 0.02 ppm (Figure 6). Significant changes in chemical shift (>0.05 ppm) are seen for Thr 614, Ala 618, Lys 621, Asp 622, Glu 626, Ala 630, and Gln 661, with the largest shifts (>0.08 ppm) observed for Phe 612, Leu 620, Val 629, and Lys 659 (Figure 6). These residues form a contiguous surface on KIX containing both hydrophobic and polar residues that define the Tax_{59-98}-binding surface (Figure 7). The binding site of Tax_{59-98} on KIX corresponds to the site recognized by human c-Jun and MLL (*20*, *21*) and is distinct from the surface utilized by phosphorylated KID (*22*) (Figure 6).

Formation of the Ternary Tax_{59-98}−pKID−KIX Complex. Sedimentation equilibrium analysis suggests that Tax_{59-98}, pKID, and KIX form a ternary complex (Figure 8). The observed mass of 21.5 ± 0.9 kDa is within 5% of the

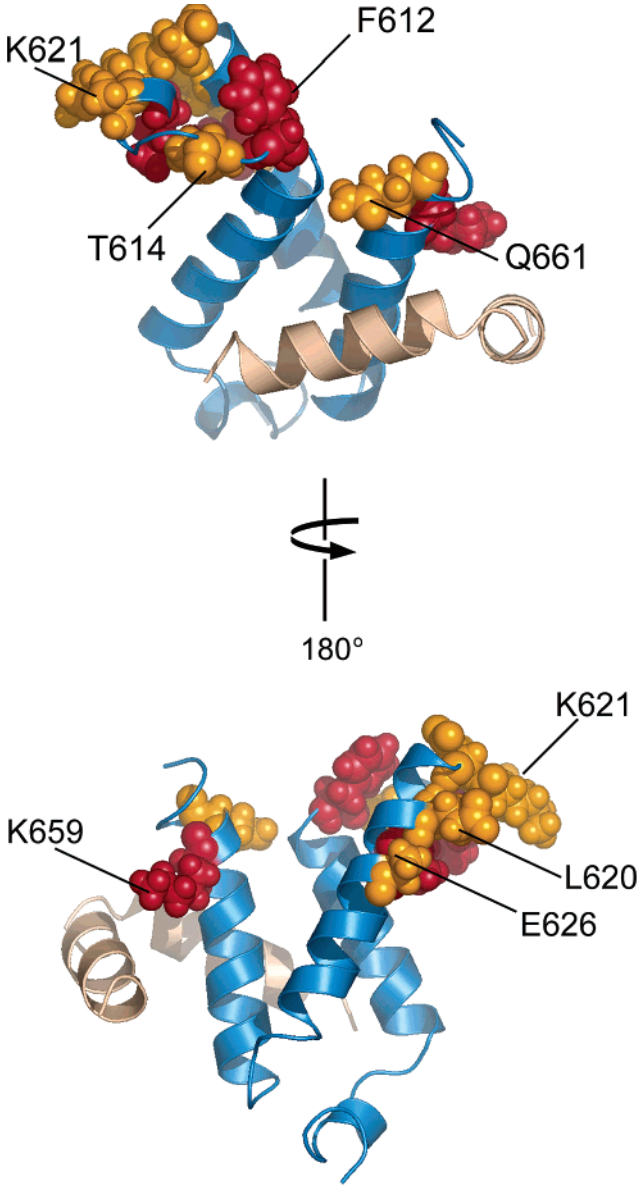

FIGURE 7: Chemical shift perturbation mapping of the Tax_{59-98}-binding site of KIX. Residues of KIX with the largest chemical shift changes form a contiguous surface of KIX that is distinct from the site occupied by pKID and corresponds instead to the site bound by human c-Jun (*20*). KIX residues with normalized chemical shift changes of 0.05−0.79 and >0.08 ppm are orange and red, respectively. The helical ribbons of KIX and pKID are blue and wheat, respectively. This image was generated with PyMol (*52*) and Protein Data Bank entry 1kdx (*22*).

expected mass (22.6 kDa) of a 1:1:1 ternary complex (Table 1). If the ternary complex did not form, then the apparent mass would be significantly lower to reflect the weight average of the Tax_{59-98}−KIX and pKID−KIX binary complexes and the unbound proteins.

Sedimentation equilibrium analysis shows that pKID and KIX associate to form a binary 1:1 complex, in accord with previous results (*22*, *26*). The observed mass of 17.9 ± 0.5 kDa is essentially identical to the expected mass of the binary complex (Table 1). pKID is a monomer in solution with an observed mass of 7.1 ± 0.3 kDa, which is within 3% of the expected mass of 6.8 kDa (Table 1). As noted above, KIX behaves essentially as a monomer (Table 1). These results indicate that the observed mass of the Tax_{59-98}−pKID−KIX

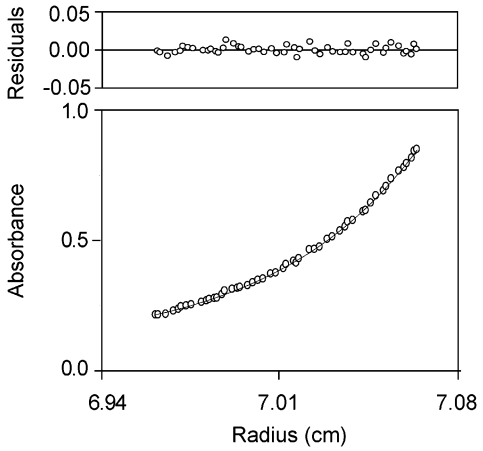

FIGURE 8: Sedimentation equilibrium analysis suggests the formation of a ternary complex of Tax_{59-98}, pKID, and KIX. The data are consistent with an ideal, single-species model with the mass expected for the 1:1:1 Tax_{59-98}−pKID−KIX complex (Table 1), as shown by the random distribution of residues.

complex is not due to self-association of the individual proteins or binary complexes.

DISCUSSION

Transcriptional activation requires the formation of numerous protein−DNA and protein−protein interactions (*39*). During CREB-mediated gene expression, the human coactivators CBP and p300 are recruited via KIX by the phosphorylated KID region of CREB (*6*, *7*). During HTLV-1 gene expression, CBP and p300 are recruited jointly by HTLV-1 Tax and human CREB (*8*, *9*). Tax promotes the binding of CREB at the atypical CRE sites of the HTLV-1 promoter and acts as a molecular bridge between the bZIP domain of CREB and the KIX domain of p300/CBP (Figure 1) (*8*, *9*). CBP and p300 may then contribute to transcriptional activation by making contacts with the general transcription machinery and by modifying the chromatin architecture surrounding the promoter (*12*−*16*, *40*). The KIX domain of CBP/p300 also binds several human transcriptional activators in addition to CREB, such as c-Jun, MLL, c-Myb, and p53, and the viral activator HIV-1 Tat (*15*, *16*, *40*). CBP and p300 are believed to be present at limiting quantities in the cell (*41*−*43*), and so, as noted previously (*17*−*19*), competition for KIX between human transcription factors and HTLV-1 Tax may have significant consequences for deregulating cellular processes that depend in part on interactions mediated by the KIX domain during gene expression.

Previous gel shift mobility studies of the competition for KIX between Tax and peptides derived from Tax suggest that the KIX-binding region includes residues 76−95 of Tax (*10*). Here we used a peptide corresponding to residues 59−98 of HTLV-1 Tax to study the Tax−KIX interaction. This peptide incorporates the region of Tax previously shown to bind KIX (*10*) and additional flanking residues that may stabilize the formation of the complex with KIX. Tax_{59-98} and KIX do form a complex, as shown with a combination of CD spectroscopy, NMR spectroscopy, and sedimentation equilibrium results. Binding is disrupted by a single-site variation of Tax_{59-98}, in which Leu 68, a candidate for participation in a hydrophobic Tax−KIX interface, is re-

```
Tax         YIDGRVIGSALQFLIPRLPSFPTQRTSKTLKVLTPPITHTT
              |   |       |           |     |
c-Jun     YGSLKPHLRAKNSDLLTSPDVGLLKLASPELERLIIQSSNGHIT
                        || |    ||   ||
MLL                  DCGNILPSDIMDFVLKNTP
```

FIGURE 9: Sequence alignments of the KIX-interacting regions of HTLV-1 Tax, human c-Jun, and human MLL. Similar residues are linked with vertical bars. Meaningful sequence similarity or a common sequence motif between Tax and the two human proteins is not apparent.

placed with the secondary structure breaking amino acid proline. The L68P substitution lies outside the region of Tax that binds KIX identified with gel shift assays (*10*), implying that the KIX-binding region of Tax likely spans a larger region than previously identified.

The CD results suggest an increase in helix content upon binding. Since KIX is an ordered, globular protein (*22*) and unbound Tax_{59-98} is devoid of significant regular helical or strand structure, it is possible that Tax_{59-98} folds to a more helical structure upon binding KIX. Coupled folding upon binding of KIX has been observed directly with NMR for the phosphorylated KID region of CREB (*22*), and has been inferred from CD studies for the activation domains from human c-Jun and HIV-1 Tat upon binding KIX (*20*, *35*).

KIX employs two distinct binding sites to recognize activation domains (*20*, *21*). One site is utilized by the phosphorylated KID region of CREB and by c-Myb (*22*, *44*), whereas the other site is utilized by c-Jun and MLL (*20*, *21*). Using NMR spectroscopy, we find that Tax recognizes the surface of KIX utilized by the human transcriptional activators MLL and c-Jun, and not that utilized by CREB.

Although HTLV-1 Tax, human c-Jun and human MLL bind the same surface of KIX, the sequences of the three transcriptional activators are not significantly similar within the KIX-interacting regions (Figure 9). The KIX-interacting regions of c-Jun and MLL share a higher degree of sequence similarity (Figure 9), but do not share an obvious common sequence motif with Tax (Figure 9). The sequences of all three peptides are predicted with AGADIR (*37*) to form helices, and quaternary interactions with KIX may impart a common structural motif that defines the mode of binding to the Tax/Jun/MLL site. Alternatively, the lack of sequence identity between Tax and Jun or MLL may reflect a structurally divergent binding mode for Tax. Further investigation with high-resolution structural methods is needed to distinguish between these possibilities.

The identification of the Tax-binding site on KIX provides a straightforward structural mechanism for Tax antagonism of human transcriptional activators that occupy the same site as Tax, and not the CREB-binding site of KIX. For example, Tax and human c-Jun compete for binding KIX (*18*), and the structural insights presented here and previously (*20*) show that this likely arises from direct competition for the same surface of KIX. Likewise, the interference of Tax with the binding of p300/CBP to p53 and MyoD (*19*, *45*−*47*) may also occur through direct competition for the Tax-binding site of KIX [and not through the CREB-binding site, as originally presumed for p53 (*45*)].

In contrast to the direct antagonism described above, Tax interference with transcription factors that bind the CREB site of KIX likely occurs through indirect mechanisms, rather than by direct competition for KIX. For example, Tax interferes with Myb-mediated transcription (*48*). NMR chemical shift mapping clearly shows that c-Myb occupies the region of KIX that is bound by CREB (*44*), and not the site shown here to be occupied by Tax. On structural grounds, therefore, it appears unlikely that Tax and c-Myb compete directly for KIX as previously supposed (*49*). Instead, our structural results are consistent with the notion that c-Myb responsive genes are suppressed by Tax indirectly through activation of NF-kB, which in turn activates expression of proteins that repress c-Myb (*48*, *50*).

The structurally distinct CREB and Tax sites suggest that KIX can bind simultaneously to Tax and CREB, which is seen here directly with sedimentation equilibrium analysis. This observation provides an additional perspective on Tax-mediated gene expression. Tax has previously been considered to act as a bridge between the bZIP domain of the HTLV-1 promoter-bound CREB and KIX to evade the cellular requirement for CREB phosphorylation during p300/CBP recruitment (*8*, *9*). However, our results show that Tax and the phosphorylated KID region of CREB can together directly bind KIX. Indeed, CREB phosphorylation markedly stabilizes the assembly of KIX, CREB, and Tax at both cellular and atypical viral CRE-containing promoters (*9*), supporting the notion that both Tax and phosphorylated CREB bind KIX during p300/CBP recruitment.

In conclusion, Tax and phosphorylated KID employ structurally distinct modes of KIX binding that allows Tax and phosphorylated CREB to jointly interact with the KIX domain of p300/CBP. Phosphorylated CREB may therefore contribute more directly to p300/CBP recruitment during Tax-mediated expression of both viral and host genes than previously recognized. Although Tax may circumvent the need for CREB phosphorylation (*8*, *9*), it is an intriguing notion that, through Tax, HTLV-1 may also take advantage of CREB phosphorylation during coactivator recruitment.

ACKNOWLEDGMENT

We thank K. M. Campbell and C. D. Rithner for valuable discussions, Y. Wei for purified pKID, S. P. Mestas for preparing the pKID expression vector, and M. Z. Gilman and R. H. Goodman for plasmids.

REFERENCES

1. Barmak, K., Harhaj, E., Grant, C., Alefantis, T., and Wigdahl, B. (2003) *Virology 308*, 1−12.
2. Bex, F., and Gaynor, R. B. (1998) *Methods 16*, 83−94.
3. Jeang, K.-T. (2001) *Cytokine Growth Factor Rev. 12*, 207−217.
4. Yoshida, M. (2001) *Annu. Rev. Immunol. 19*, 475−496.
5. Pise-Masison, C. A., Radonovich, M., Mahieux, R., Chatterjee, P., Whiteford, C., Duvall, J., Guillerm, C., Gessain, A., and Brady, J. N. (2002) *Cancer Res. 62*, 3562−3571.
6. Chrivia, J. C., Kwok, R. P., Lamb, N., Hagiwara, M., Montminy, M. R., and Goodman, R. H. (1993) *Nature 365*, 855−859.
7. Parker, D., Ferreri, K., Nakajima, T., LaMorte, V. J., Evans, R., Koerber, S. C., Hoeger, C., and Montminy, M. R. (1996) *Mol. Cell. Biol. 16*, 694−703.
8. Kwok, R. P. S., Laurance, M. E., Lundblad, J. R., Goldman, P. S., Shih, H., Conner, L. M., Marriot, S. J., and Goodman, R. H. (1996) *Nature 380*, 642−646.
9. Giebler, H. A., Loring, J. E., van Orden, K., Colgin, M. A., Garrus, J. E., Escudero, K. W., Brauweiler, A., and Nyborg, J. K. (1997) *Mol. Cell. Biol. 17*, 5156−5164.
10. Harrod, R., Tang, Y., Nicot, C., Lu, H. S., Vassilev, A., Nakatani, Y., and Giam, C.-Z. (1998) *Mol. Cell. Biol. 18*, 5052−5061.
11. Yan, J., Garrus, J., Giebler, H. A., Stargell, L. A., and Nyborg, J. K. (1998) *J. Mol. Biol. 281*, 395−400.

12. Lu, H., Pise-Masison, C. A., Fletcher, T. M., Schiltz, R. L., Nagaich, A. K., Radonovich, M., Hager, G., Cole, P. A., and Brady, J. N. (2002) *Mol. Cell. Biol. 22*, 4450−4462.
13. Georges, S. A., Giebler, H. A., Cole, P. A., Luger, K., Laybourn, P. J., and Nyborg, J. K. (2003) *Mol. Cell. Biol. 23*, 3392−3404.
14. Kashanchi, F., Duvall, J. F., Kwok, R. P. S., Lundblad, J. R., Goodman, R. H., and Brady, J. N. (1998) *J. Biol. Chem. 273*, 34646−34652.
15. Goodman, R. H., and Smolik, S. (2000) *Genes Dev. 14*, 1553−1577.
16. Chan, H. M., and La Thangue, N. B. (2001) *J. Cell Sci. 114*, 2363−2373.
17. Suzuki, T., Uchida-Toita, M., and Yoshida, M. (1999) *Oncogene 18*, 4137−4143.
18. Van Orden, K., Yan, J. P., Ulloa, A., and Nyborg, J. K. (1999) *Oncogene 18*, 3766−3772.
19. Ariumi, Y., Kaida, A., Lin, J.-Y., Hirota, M., Masui, O., Yamaoka, S., Taya, Y., and Shimotohno, K. (2000) *Oncogene 19*, 1491−1499.
20. Campbell, K. M., and Lumb, K. J. (2002) *Biochemistry 41*, 13956−13964.
21. Goto, N. K., Zor, T., Martinez-Yamout, M., Dyson, H. J., and Wright, P. E. (2002) *J. Biol. Chem. 277*, 43168−43174.
22. Radhakrishnan, I., Pérez-Alvarado, G. C., Parker, D., Dyson, H. J., Montminy, M. R., and Wright, P. E. (1997) *Cell 91*, 741−752.
23. Ernst, P., Wang, J., Huang, M., Goodman, R. H., and Korsmeyer, S. J. (2001) *Mol. Cell. Biol. 21*, 2249−2258.
24. Zuiderweg, E. R. P. (2002) *Biochemistry 41*, 1−7.
25. Schnölzer, M., Alewood, P., Jones, A., Alewood, D., and Kent, S. B. H. (1992) *Int. J. Pept. Protein Res. 40*, 180−193.
26. Mestas, S. P., and Lumb, K. J. (1999) *Nat. Struct. Biol. 6*, 613−614.
27. McIntosh, L. P., and Dahlquist, F. W. (1990) *Q. Rev. Biophys. 23*, 1−38.
28. Berkowitz, L. A., and Gilman, M. Z. (1990) *Proc. Natl. Acad. Sci. U.S.A. 87*, 5258−5262.
29. Edelhoch, H. (1967) *Biochemistry 6*, 1948−1954.
30. Laue, T. M., Shah, B. D., Ridgeway, T. M., and Pelletier, S. L. (1992) in *Analytical Ultracentrifugation in Biochemistry and Polymer Science* (Harding, S. E., Rowe, A. J., and Horton, J. C., Eds.) pp 90−125, The Royal Society of Chemistry, Cambridge, U.K.
31. Kay, L., Keifer, P., and Saarinen, T. (1992) *J. Am. Chem. Soc. 114*, 10663−10665.
32. Johnson, B. A., and Blevins, R. A. (1994) *J. Biomol. NMR 4*, 603−614.
33. Delaglio, F., Grzesiek, S., Vuister, G. W., Zhu, G., Pfeifer, J., and Bax, A. (1995) *J. Biomol. NMR 6*, 277−293.
34. Radhakrishnan, I., Pérez-Alvarado, G. C., Parker, D., Dyson, H. J., Montminy, M., and Wright, P. E. (1999) *J. Mol. Biol. 287*, 859−865.
35. Vendel, A. C., and Lumb, K. J. (2003) *Biochemistry 42*, 910−916.
36. Creighton, T. E. (1993) *Proteins: Structures and Molecular Properties*, W. H. Freeman and Co., New York.
37. Muñoz, V., Cronet, P., López-Hernández, E., and Serrano, L. (1996) *Folding Des. 1*, 167−178.
38. Serrano, L. (2000) *Adv. Protein Chem. 53*, 49−85.
39. Orphanides, G., and Reinberg, D. (2002) *Cell 108*, 439−451.
40. Vo, N., and Goodman, R. H. (2001) *J. Biol. Chem. 276*, 13505−13508.
41. Kamei, Y., Xu, L., Heinzel, T., Torchia, J., Kurokawa, R., Gloss, B., Lin, S. C., Heyman, R. A., Rose, D. W., Glass, C. K., and Rosenfeld, M. G. (1996) *Cell 85*, 403−414.
42. Horvai, A. E., Xu, L., Korzus, E., Brard, G., Kalafus, D., Mullen, T. M., Rose, D. W., Rosenfeld, M. G., and Glass, C. K. (1997) *Proc. Natl. Acad. Sci. U.S.A. 94*, 1074−1079.
43. Hottiger, M. O., Felzien, L. K., and Nabel, G. J. (1998) *EMBO J. 17*, 3124−3134.
44. Zor, T., Mayr, B. M., Dyson, H. J., Montminy, M. R., and Wright, P. E. (2002) *J. Biol. Chem. 277*, 42241−42248.
45. Van Orden, K., Giebler, H. A., Lemasson, I., Gonzales, M., and Nyborg, J. K. (1999) *J. Biol. Chem. 274*, 26321−26328.
46. Riou, P., Bex, F., and Gazzolo, L. (2000) *J. Biol. Chem. 275*, 10551−10560.
47. Pise-Masison, C. A., Mahieux, R., Radonovich, M., Jiang, H., and Brady, J. N. (2001) *J. Biol. Chem. 276*, 200−205.
48. Nicot, C., Mahieux, R., Opavsky, R., Cereseto, A., Wolff, L., Brady, J. N., and Franchini, G. (2000) *Oncogene 19*, 2155−2164.
49. Colgin, M. A., and Nyborg, J. K. (1998) *J. Virol. 72*, 9396−9399.
50. Nicot, C., Mahieux, R., Pise-Masison, C. A., Brady, J. N., Gessain, A., Yamaoka, S., and Franchini, G. (2001) *Mol. Cell. Biol. 21*, 7391−7402.
51. Mayr, B. M., and Montminy, M. (2001) *Nat. Rev. Mol. Cell Biol. 2*, 599−609.
52. DeLano, W. L. (2003) http://www.pymol.org.

BI0353023